Journal of Applied Mechanics and Technical Physics, Vol. 37, No. 6, 1996

AERO-OPTICS OF FLOWS BEHIND THE NOZZLE BANKS OF FAST-FLOW LASERS

V. M. Mal'kov

UDC 533.697+532.517.4

1. Introduction. The aero-optical effect (wavefront aberrations in the light beam) occurs when the beam travels through density inhomogeneities of an air medium and is due to changes in the refractive index which is linearly related to the density of this medium. This is the case when radiation passes through both regular structures (shock systems and slip surfaces) [1] and turbulent structures (wakes, boundary and shear layers) [2, 3]. The case where the scale of disturbances, for example, turbulent oscillations, is smaller than the beam aperture is considered in aero-optics. Unlike aero-optics, in atmospheric optics the opposite situation is considered: the disturbance is larger than the beam aperture.

Consideration of aero-optical problems as a separate discipline is due to a large extent to the invention of lasers. Numerous problems have arisen concerning radiation passage, for instance, through the boundary layer when lasers are mounted on board an aircraft [4, 5]. The use of optical guidance systems on supersonic vehicles has led to the second type of problems: correct interpretation of the signal from a radiation detector. Before entering the detector window, the beam passes through a shock wave and a turbulent mixing layer of external cold gas flow that cools the window. This means that the signal depends in time on the conditions formed in the flow around this vehicle, which should be taken into account for giving commands to control systems [6, 7].

The problems of aero-optics are of great importance for fast-flow laser systems — chemical (CL) and gas-dynamic (GDL) lasers in which supersonic gas pumping is used [8–10]. Multinozzle banks (arrays) are used as nozzles in CL and GDL and, as a result, the wakes, expansion fans, and shock systems exist inevitably in flow past the nozzle-bank base in the resonator cavity. This means that radiation is formed in a medium with substantially inhomogeneous density, and, hence, the wave front at the resonator exit is not ideal — plane, i.e., radiation scattering is higher than diffraction scattering [11]. Therefore, studies of these problems should be aimed at establishing relations between the flow parameters in the resonator and the beam quality. The problem of increasing the efficiency of the laser system can be solved only on this basis.

The degree of aberration of a plane wave front upon radiation passage through a medium determines the optical quality of the medium. In the present paper (which is a continuation of [12, 13]), the optical quality of flow behind blade- and screen-nozzle banks used in CL and GDL is studied, and the effect of the turbulent characteristics of flows behind them on the optical quality of flow as a whole is determined.

As was noted in [12], to interpret the results of optical measurements, the data on the gas-dynamic structure of the flows to be studied should be involved. The averaged flow characteristics for all tested nozzle banks obtained by probing methods are presented in [14–16], and the data on the intensity of the turbulent oscillations downstream of the nozzle banks are given in [17]. However, the most important aspects, which are necessary to explain optical results are described in the present paper.

2. Experimental Setup. Measurement Techniques. The experimental conditions are described in [12]. Here we only mention the basic conditions, including additional ones. The experiments were performed in a small-scale wind tunnel (51 × 56 mm test section), with blade and screen nozzle banks employed as its nozzle. The test section was modified for this series of experiments: it was equipped with additional windows, and, therefore, optical measurements were performed at a distance of up to 250 mm from the nozzle exit

Institute of Theoretical and Applied Mechanics, Siberian Division, Russian Academy of Sciences, Novosibirsk 630090. Translated from Prikladnaya Mekhanika i Tekhnicheskaya Fizika, Vol. 37, No. 6, pp. 26–34, November–December, 1996. Original article submitted July 21, 1995.

 0021-8944/96/3706-0794 $15.00

(up to 90 mm in [12]). The flow regime in the wakes was turbulent: the Reynolds number based on the flow parameters at the nozzle exits was $\mathrm{Re} = (0.85\text{–}5.3) \cdot 10^6$.

Nozzle Banks. Screen-Nozzle Banks for GDL were first suggested in [8]. The idea was then proposed to use complicated modifications of them in mixing lasers [9] and in CL [10]. In the general case, a screen-nozzle bank is a grid of closely positioned conical or contoured micronozzles, which are identical for GDL or are of two types for mixing lasers or for CL. In the present work, we used only the arrays with identical micronozzles ($\sim$ 130 in each array). The micronozzles had a 1-mm throat section, expansion ratio 25, and the same subsonic part. The conical-nozzle arrays were made in two variants: with the nozzle half-angle $\alpha = 10$ and 20°. The arrays with contoured micronozzles (the profile was calculated by the method of characteristics) were made as follows. A contour designed for a larger degree of expansion was truncated, so that the nozzle expansion ratio was the same as for conical nozzles (25). The descent flow angle was not zero in this case, but amounted to 5°, and the supersonic part of the contour was 11 mm long (11 mm for conical nozzles with $\alpha = 10°$ and 5.4 mm for those with $\alpha = 20°$). The new arrays were fabricated in two variants as well: in the first variant, in mounting the array in the gas-dynamic tract the rows of micronozzles were located parallel to the optical axis of the experimental setup ($\psi = 0$, unskewed screen-nozzle bank), and in the second variant they were not parallel to the optical axis ($\psi = 13°$, skewed screen-nozzle bank).

We used the same *blade-nozzle banks* as in [12], where they are described in detail. Each array consisted of four blade nozzles formed by three full blades contoured on both sides and by two lateral blades contoured from one side. The blade contours were calculated by the method of characteristics for the Mach number equal to 5 (throat section 0.5 mm and adiabatic index 1.4). The blade-edge thickness t (from 0.15 to 1 mm) and the descent flow angle α (from 0 to 4°) were varied in the experiments.

Measurements. The Schlieren technique with a spark light source was employed for flow visualization. The averaged flow parameters were found from the measurements of total- and static-pressure fields, which were performed by appropriate probes [14, 16]. The technique of hot-wire measurements of the fluctuating flow parameters is presented in [17].

In optical studies, the focal-spot method (the far-field power-in-the-bucket method) was used. Its essence is measurement of the intensity of light collected by a lens in the far radiation region in the central spot, i.e., in the focal spot. The principal scheme of equipment and the description of the operation system are given in [12]. The differential scheme was used. The probing-laser beam was split into two: one beam passed through the medium to be examined, and the other arrived directly at a radiation detector. The difference in the signals from these detectors which is caused by the presence of inhomogeneous flow in the resonator cavity was registered.

In contrast to previously published papers (for example, [4]) in which wide-aperture beams were commonly used for probing and the measurement result was, in fact, averaged over the entire aperture of the resonator, we used a beam with a comparatively small diameter. This approach allowed us to have a certain spatial resolution during the measurements and to trace the effect of separate elements of the flow structure, primarily, the effect of the evolution of turbulent structures, on its optical quality. (At the same time, the beam could not be too thin and must be much larger than the dimensions of turbulent vortices for averaging of results over the beam diameter to be representative.)

Interferometry is also often used in aero-optics [4]. In this case, information on wavefront aberrations is obtained in the near radiation zone. Using the Strehl ratio [11], one can calculate, for example, the radiation intensity in the central spot of the far zone. In fact, the Strehl ratio relates the two methods. However, when studying the effect of the fluctuating flow characteristics on its optical quality, one has to obtain many instantaneous interferograms and average the results properly. The data obtained by the two methods were compared in [18], where it was noted that dozens of photographs are needed for representative averaging. Obviously, processing of so many interferograms to obtain a single point is a cumbersome procedure. Otherwise, there is a great scatter of points. It was noted in [19] that the standard scatter of points obtained from instantaneous interferograms is more than 20%. Simultaneously, the error in the measured r.m.s. phase deviation $\Delta\bar{\varphi}$ leads to large errors in the intensity values, since $\Delta\bar{\varphi}$ is the exponent factor in the Strehl ratio. Therefore, it is more convenient to use the focal-spot method as a direct method to reveal the effect of the

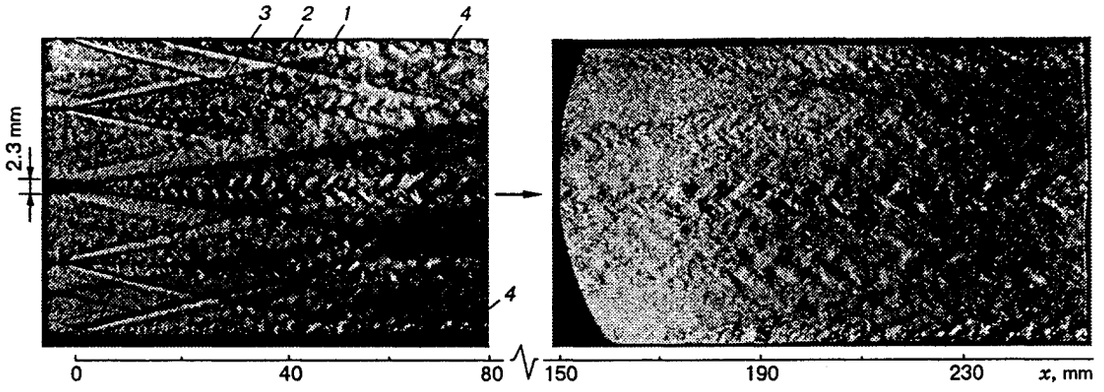

Fig. 1

basic physical mechanisms on light scattering in the flow.

3. Experimental Results. Discussion. *Blade Nozzles.* The asymptotic expression

$$\Delta\bar{I} = (I_0 - I)/I_0 \sim x\rho^2 \tag{3.1}$$

was obtained in [12] for the nondimensional intensity of light scattered by turbulent wakes behind flat blades. Here I_0 and I are the intensities of incident light and of light transmitted through the medium, x is the distance from the nozzle exit, ρ is the flow density, and $\Delta\bar{I}$ is unity minus the Strehl number, which is commonly used as an estimate of the flow quality. The estimate of (3.1) easily follows from the Strehl ratio and from the expression for phase variation in the light beam (that passed through a turbulent layer of thickness L) derived in [2] for homogeneous and isotropic turbulence:

$$\Delta\varphi = (2\pi/\lambda)\sqrt{\Lambda L}\,\bar{\rho}'\,\bar{\rho}. \tag{3.2}$$

Here Λ is the turbulence scale, λ is the wavelength, $\bar{\rho}' = \rho'/\rho$ is the nondimensional intensity of density fluctuations, and $\bar{\rho}$ is the flow density referred to the medium density under standard conditions.

For estimation, we took into account the following experimental data: in a plane free wake after the initial section $\bar{\rho}'$ is practically a constant quantity [20], $\Lambda \sim L$ for boundary and mixing layers [21, 22] (for various cases, the proportionality coefficient varies from 0.1 to 0.5 in different papers), the wake thickness $L(x)$ is proportional to $\sqrt{x}$ (the complete dependence $L(x)$ in self-similar far-wake variables is presented in [12, 14]).

Relation (3.1) was validated by the $\Delta\bar{I}$ measurements in the first window ($x = 90$ mm). This shows that the φ variations are primarily determined by the turbulent character of flow and by an increase in the wake thickness. Nevertheless, the behavior of $\Delta\bar{I}$ in the regions $x > 100$ mm is also of interest, since for powerful laser systems, the downstream resonator size can be more than 200 mm. However, farther downstream the interaction of wakes is inevitable as $L(x)$ increases, and they cannot be considered free wakes.

Figure 1 shows the flow pattern behind a blade-nozzle bank obtained in two sequentially positioned windows (the distance from the nozzle exit is given beneath the photographs). To show more clearly the flow details behind a single blade, a blade with a very thick edge ($t = 2.3$ mm) was placed at the center of the nozzle array, and two other blades are commonly used ($t = 0.35$ mm). In the first window, one can clearly see the vortex structure of individual wakes 1 which is transformed into a large-scale vortex structure at the end of the window, an expansion-wave system 2 arising upon flow deflection on the vane edges (light regions), a shock wave system 3 where the flow is again deflected parallel to the axis (dark lines), and boundary layers 4 on the walls.

It is the effect of shock and expansion waves on the wake that makes this problem different from the free-wake problem usually considered in aerodynamics (see, for example, [20]). The conducted measurements have shown, however, that the flow in the wake is also self-similar in our case (within the measurement accuracy), i.e., the parameter distributions across the wake presented in the so-called far-wake coordinates

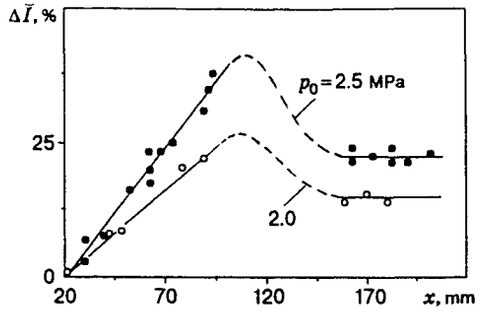

Fig. 2

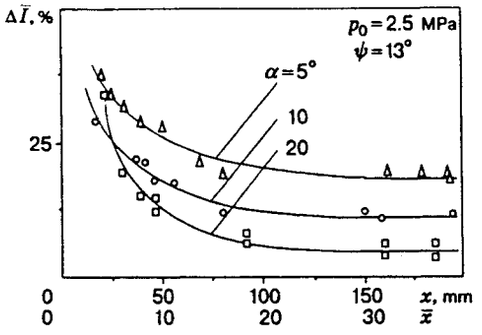

Fig. 3

coincide in all cross sections. This is caused by the fact that the expansion region is always closed with a shock. Simultaneous actions of these two factors on the wake are mutually compensated. The action of a shock alone leads to violation of the self-similarity in the wake, i.e., to its thickening. Thus, it is incorrect to calculate the difference of optical paths in the flows downstream of multinozzle arrays, taking into account only the presence of the shock, as was done in [23]. Neither expansion waves nor wakes were taken into account in [8, 23].

The flow structure becomes different in the second window. At approximately $x = 200$ mm, the adjacent wakes begin to overlap and interfere with each other. Large-scale vortices are destroyed and the entire flow is turbulized. From an optical point of view, the flow becomes practically uniform and has an obviously smaller turbulence scale, as compared with that registered in the wake at the end of the first window. However, the measured averaged-parameter distributions still do register the typical inhomogeneities that are caused by the presence of wakes, i.e., complete flow mixing has not yet occurred from the viewpoint of gas dynamics.

As follows from Fig. 2, where the data for two values of stagnation pressure p_0 are presented, the behavior of $\Delta\bar{I}(x)$ along the entire channel clearly reflects the character of the flow evolution: after the linear growth up to $x = 90$ mm, the $\Delta\bar{I}(x)$ values drop rapidly in the region $x \approx 200$ mm. The qualitative change of the turbulence scale registered in the photographs explains this result: this follows from (3.2). However, for quantitative estimates, one should measure the density-fluctuation intensity, since $\bar{\rho}' \approx$ const was obtained in [20] for a free wake and is not observed in the region $x = 200$ mm. Formula (3.2) holds for uniform and isotropic turbulence, but the effect of large-scale vortices as compared with small-scale ones is more profound for nonuniform and nonisotropic turbulence, as is shown in [24].

The results of Fig. 2 are common for all blade-nozzle banks with various t and α. No differences were found within the accuracy of our measurements, though, as will be shown below, the results for screen-nozzle banks exhibit the effect of α. Apparently, the range of α variation in the case of blade nozzles is small, and, moreover, these models are made such that t increases with α. The action of these factors is opposite: an increase in α decreases $\bar{\rho}'$, and an increase in t increases Λ.

Unfortunately, no experimental points were obtained in the region $100 \leqslant x \leqslant 150$ mm (because of a lintel between the windows). Therefore, the shape of $\Delta\bar{I}(x)$ is hypothetical here. But an increase in $\Delta\bar{I}(x)$ after $x = 100$ mm can be naturally assumed, since the wakes in the first window do not yet merge, and the wake thickness and, hence, Λ will obviously continue to increase. It is also clear that the curve $\Delta\bar{I}(x)$ will deflect earlier if the distance between the adjacent blades is reduced (taking a smaller throat section for nozzles retaining the same degree of expansion, i.e., the mean flow density). Apparently, the scale of turbulence in the wake-mixing region will be less: mixing will begin at smaller absolute dimensions of the wakes. This mechanism of rapid formation of turbulent flow which is uniform from the optical viewpoint is responsible for the results obtained for screen-nozzle banks.

Screen-Nozzle Banks. From Fig. 3, which shows $\Delta\bar{I}(x)$ along the channel for arrays with different descent flow angles, it follows that the portion of scattered radiation is reduced with increasing α. This fact, along with the general qualitative shape of the curves, explains the data on the fluctuation intensity of the

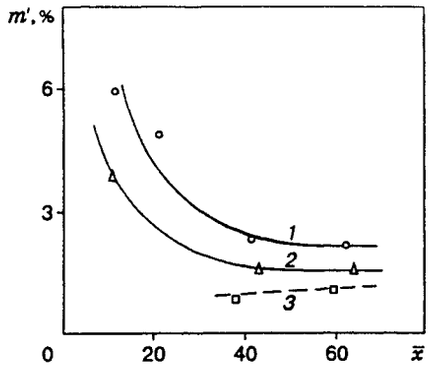

Fig. 4

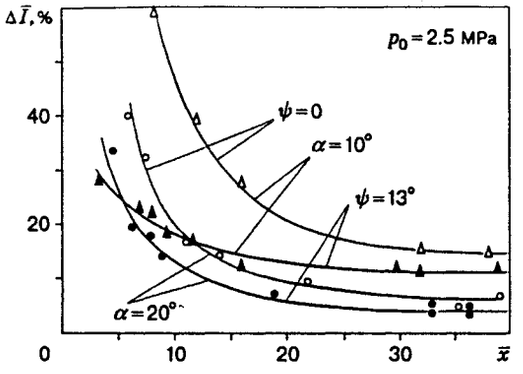

Fig. 5

mass flow $m'(\bar{x})$ in Fig. 4. This figure shows the results for an array with $\alpha = 10°$ (1) and for an array with $\alpha = 20°$ (2), and also the points for a conventional aerodynamic nozzle (3). Hereinafter $\bar{x} = x/d_e$ (d_e is the exit diameter of a micronozzle in an array, $d_e = 5$ mm). Comparison of the results presented shows that for blade-nozzle banks, the behavior of $\Delta\bar{I}(x)$ is due, first of all, to the changes of the turbulent scale in the flow, whereas the determining quantity for screen-nozzle banks is the intensity of density fluctuations $\bar{\rho}'$, since the qualitative behavior of the curves $\Delta\bar{I}(x)$ and $m'(\bar{x})$ is the same. (The hot-wire signal is known to be proportional to m', but since the density fluctuations make the major contribution to the signal, ρ' and m' have a similar behavior. It is possible, in principle, to distinguish ρ' and velocity under special assumptions.)

Let us consider the behavior of the turbulence scale in the region considered. One can see from the flow photographs taken downstream of screen-nozzle banks (which are given in [12]) that the flow that is uniform from the optical point of view with a single scale Λ is formed at distances of $\bar{x} = 10$. The study [25] of the Λ values behind hole screens shows that Λ changes weakly along the flow (experimental points were obtained up to $\bar{x} \leqslant 40$) and depends on the screen parameters. Therefore, in our case the values of Λ in the flow should be assumed equal for arrays with the same d_e and with the same nozzle packing, and $\Lambda \approx$ const along the channel. Owing to this fact and to the behavior of $m'(\bar{x})$, the value of $\Delta\bar{I}(x)$ in Fig. 3 does not change after $\bar{x} \approx 20$–30. However, complete mixing of wakes and individual flows from the viewpoint of gas dynamics occurs much farther downstream, which was also noted above for blade-nozzle banks. Therefore, the difference in the results for screen-nozzle banks with differently arranged micronozzle rows relative to the axis (different ψ) is preserved far downstream (Fig. 5). The different jet-flow geometry is especially noticeable in the initial section $\bar{x} \leqslant 10$, but the difference in the values of $\Delta\bar{I}(x)$ for arrays with $\psi = 0$ and 13° is also observed after $\bar{x} \geqslant 30$.

Figure 6 shows the averaged density fluctuations in the flow behind conical screen-nozzle banks (points 1 and 2 refer to $\alpha = 20$ and 10°, respectively); $\Delta\tilde{\rho}$ is the maximum deviation (outside the boundary layer) of the time-averaged density changing over the cross section from the mean density value $\tilde{\rho}$ in this section, i.e., $\Delta\tilde{\rho}$ is determined directly by the jet-like character of the averaged flow rather than by the fluctuation characteristics of the mixing regions. The data were obtained from the results of measurements with total- and static-pressure probes [15, 16]. For comparison, this figure shows the data from [8] for $\alpha = 10°$ obtained on the basis of interferometric measurements. One can see that $\Delta\tilde{\rho}/\tilde{\rho}$ decreases to 1–1.5% in the region $\bar{x} = 80$–100, i.e., the flow becomes uniform in the gas-dynamic sense and, hence, the values of $\Delta\bar{I}(x)$ are no longer different for arrays with different ψ.

It is commonly known that the flow downstream of screen-nozzle banks has better optical quality for $\psi \neq 0$. Without solving the gas-dynamic problem, only from the array geometry (with densely packed nozzles) it follows that the first and optimum displacement angle of the optical axis from the nozzle rows is $\tan\psi = d_e/L_p$ (L_p is the array dimension along the resonator). The results presented here indicate that the degree of improvement of the optical quality of flow is not the same along the test section. In addition, no worse effect (in the sense of reduction of the amount of light scattered on turbulent inhomogeneities) can be

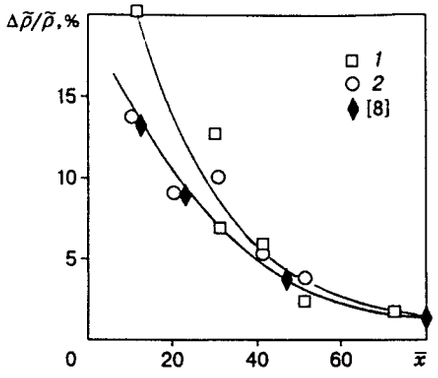

Fig. 6

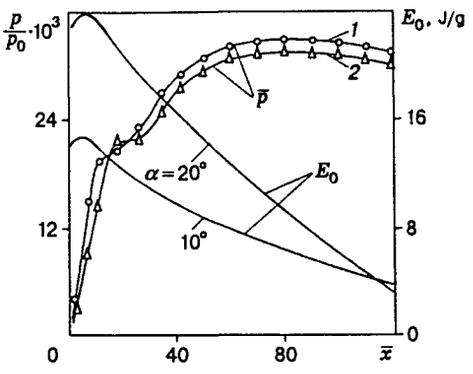

Fig. 7

achieved by changing the nozzle geometry and affecting the turbulence characteristics. From the viewpoint of the optical properties of flow, the arrays with contoured micronozzles with descent flow angle $\alpha = 0$ are the least effective.

As for conical arrays, we note the following. In agreement with the numerical estimates of [8], the arrays with $\alpha = 10°$ are commonly considered the most suitable. This conclusion is based on the fact that the total-pressure losses caused by flow deflection and jet mixing at $\alpha > 10°$ are large. However, the experimental data on pressure P_f recovery in a rectangular channel of constant cross section (the simplest type of a diffusor) obtained in [15, 16] have shown that the P_f value for an array with $\alpha = 20°$ is very close to that in the case of $\alpha = 10°$. This also happens, because the effective Mach number at the diffusor entrance in the flow behind the nozzles with $\alpha = 20°$ is slightly smaller than behind the nozzle with $\alpha = 10°$, i.e., the total-pressure losses certainly exist, but they are not large.

Figure 7 demonstrates the distribution of the static pressure p over the channel wall for two cases: the usual large-diameter nozzle (curve 1) and a screen-nozzle bank (curve 2) (the sum of the throat areas of micronozzles in the bank is the same as the throat area of the usual nozzle) were used in the experiment. The curves are shown for the case where the pseudoshock region which can be shifted using the counterpressure upon exhaust, which is controlled by the ejector, begins near the nozzle exit, i.e., when the maximum value of P_f is reached. The maximum difference in the values of $\bar{p}$ is 10%, and, therefore, the starting pressures of the device for the two cases differ by less than 10% (if the same diffusor is used). The total-pressure fields at the diffusor exit are given in [16], and they are only slightly different as well.

In addition, Fig. 7 shows the calculated amount of the stored energy E_0 in flow behind a screen-nozzle bank. It can be released in the form of radiation with allowance for the resonator efficiency for conditions of homogeneous CO_2-GDL. Two cases are compared where a conical array with $\alpha = 10$ and 20° is used as a nozzle. The calculation technique is well known [26]: the one-dimensional inviscid gas dynamics is solved together with the four-temperature kinetic model. The conditions (composition of a water-containing mixture, temperature, and pressure) are fairly standard for GDL and are presented in [15]. Obviously, the use of arrays with large angles of nozzle expansion is more advantageous, since freezing of vibrational energy and separation between vibrational and translational temperatures in the nozzle-throat region are more efficient. In this case, nearly a twofold gain is obtained if the resonator is positioned comparatively close to the nozzle exit. This determines the importance of the presented results of measurement of the optical quality of flow. For screen-nozzle banks with displaced nozzle axis ($\psi \neq 0$), the resonator can be placed not at distances of $\bar{x} = 80$–100 (according to the recommendations of [8, 23]), where the level of fluctuations of the mean parameters is low, but at distances of $\bar{x} = 20$–30, where the level of turbulent-fluctuation intensity is low. This is important, since the portion of E_0 here is not yet much different from the maximum possible values, while at distances of $\bar{x} = 80$–100 it is only a small portion of the maximum energy.

In conclusion, we shall formulate the basic results. The experiments conducted prove that aberrations of plane wave fronts in flow downstream of multinozzle arrays are caused by the presence of turbulent wakes rather than by the shock-wave structure of flow, as was assumed in [8, 9, 23]. The qualitative relation between the basic flow parameters and the phase shift is determined by formula (3.2), despite the fact that it was derived for homogeneous and isotropic turbulence. The flow character and the turbulence parameters, and, hence, the optical quality of flow can be affected by the choice of nozzles, their contouring and arrangement in an array. In designing multinozzle arrays, one should attempt to obtain small-scale flow turbulence, even if the flow is completely turbulent.

REFERENCES

1. H. W. Liepmann and A. Roshko, *Elements of Gas-Dynamics*, Wiley, New York (1957).
2. G. Sutton, "Effect of turbulent fluctuations in an optically active fluid medium," *AIAA J.*, **7**, No. 9, 1737–1743 (1969).
3. G. Sutton, "Aero-optical foundations and applications," *AIAA J.*, **23**, No. 10, 1525–1537 (1985).
4. K. Gilbert and L. Otten (eds.), *Progress in Astronautics and Aeronautics: Aero-Optical Phenomena*, AIAA, New York (1982), Vol. 80.
5. A. E. Fuhs, "Overview of aero-optical phenomena," in: A. Fuhs and B. Fuhs (eds.), *Wavefront Distortions in Power Optics*, SPIE, Washington (1981), Vol. 293.
6. A. D. Kathman, L. C. Brooks, and D. A. Kalin, "A time-integrated image model for aero-optics analysis," AIAA Paper No. 92–2793, New York (1992).
7. G. Haveren, "Optical wave front variance," AIAA Paper No. 92–0694, New York (1992).
8. D. A. Russel, S. E. Neice, and P. N. Rose, "Screen nozzles for gas-dynamic lasers," *AIAA J.*, **13**, No. 5, 593–599 (1975).
9. P. E. Cassady and I. Newton, "A new mixing laser," AIAA Paper No. 76–343, New York (1976).
10. S. W. Zelazny, W. A. Chambers, W. F. van Tassell, and W. F. Brandkamp, "Medium inducted phase aberration in continuous wave hydrogen fluoride chemical lasers," in: A. Fuhs and B. Fuhs (eds.), *Wavefront Distortions in Power Optics*, SPIE, Washington (1981), Vol. 293.
11. M. Born and E. Wolf, *Principles of Optics*, Macmillan, New York (1964).
12. M. G. Ktalkherman and V. M. Mal'kov, "Aero-optics of nozzle arrays of gas-dynamic lasers," *Prikl. Mekh. Tekh. Fiz.*, **34**, No. 6, 20–28 (1993).
13. V. M. Mal'kov and M. G. Ktalkherman, "Some aspects of aero-optics of GDL nozzle banks," AIAA Paper No. 94–2447, New York (1994).
14. M. G. Ktalkherman, V. M. Mal'kov, and N. A. Ruban, "Flowfield characteristics downstream of blade-nozzle banks," Report No. 2090, Inst. Theor. Appl. Mech., Sib. Div., USSR Acad. Sci., Novosibirsk (1991).
15. M. A. Anikin, M. G. Ktalkherman, V. M. Mal'kov, and A. P. Sinitsyn, "Dependence of flowfield parameters downstream of screen nozzles on the divergence angle of an individual micronozzle," in: *Gas-Dynamics of* GDL *Ducts* (Collected scientific papers) [in Russian], Inst. Theor. Appl. Mech., Sib. Div., USSR Acad. Sci. (1987).
16. V. K. Baev, M. G. Ktalkherman, V. M. Mal'kov, and A. N. Ruban, "Flowfield parameters and pressure recovery in a rectangular channel downstream of screen nozzles," in: *Gas-Dynamics of* GDL *Ducts* (Collected scientific papers) [in Russian], Inst. Theor. Appl. Mech., Sib. Div., USSR Acad. Sci. (1982).
17. V. N. Zinov'ev, M. G. Ktalkherman, V. A. Lebiga, and V. M. Mal'kov, "Mean and turbulent characteristics of supersonic flow in a wind tunnel with a screen nozzle," *Izv. Sib. Otd. Akad. Nauk SSSR, Ser. Tekh. Nauk*, No. 5, 37–42 (1989).
18. D. W. Bogdanoff, "Optical quality of supersonic jets of various gases," *Appl. Opt.*, **21**, No. 5, 893–903 (1982).
19. G. W. Sutton, "Hypersonic interceptor aero-optics performance predictions," *J. Spacecraft Rocket.*, **31**, No. 4, 592–599 (1994).

20. A. Demetriades, "Observation on the transition process of two-dimensional supersonic wakes," *AIAA J.*, **9**, No. 11, 2128–2134 (1971).
21. R. G. Butt, "Turbulent mixing of passive and chemically reacting species in a low-speed shear layer," *J. Fluid Mech.*, **82**, 53–60 (1977).
22. G. Sutton, "Optical image through aircraft turbulent boundary layers," in: K. Gilbert and L. Otten (eds.), *Progress in Astronautics and Aeronautics*, AIAA, New York (1982), Vol. 80.
23. T. S. Vaidyanathan and D. A. Russel, "Wave-generated disturbance downstream of nozzle array," *AIAA J.*, **23**, No. 5, 749–757 (1985).
24. C. R. Truman, "The influence of turbulent structure on optical phase distortion through turbulent shear flows," AIAA Paper No. 92–2817, New York (1992).
25. V. S. Kalizhnikov, "One-dimensional characteristics of turbulence behind various grids," in: *Thermo-Hydro-Gas-dynamics of Turbulent Flows* (Collected scientific papers) [in Russian], Inst. Thermal Phys., Sib. Div., USSR Acad. Sci. (1986).
26. S. A. Losev, *Gasdynamic Lasers* [in Russian], Nauka, Moscow (1977).